We are IntechOpen,
the world's leading publisher of
Open Access books
Built by scientists, for scientists

6,900
Open access books available

186,000
International authors and editors

200M
Downloads

Our authors are among the

154
Countries delivered to

TOP 1%
most cited scientists

12.2%
Contributors from top 500 universities

CLARIVATE ANALYTICS
**BOOK
CITATION
INDEX**
INDEXED

WEB OF SCIENCE™

Selection of our books indexed in the Book Citation Index
in Web of Science™ Core Collection (BKCI)

Interested in publishing with us?
Contact book.department@intechopen.com

Numbers displayed above are based on latest data collected.
For more information visit www.intechopen.com

Time-Resolved Fluorescence Spectroscopy with LabView

Edgard Moreno, Porfirio Reyes and José M. de la Rosa
Instituto Politécnico Nacional
México

1. Introduction

1.1 Fluorescence phenomenon

The absorption and subsequent emission of light by organic and inorganic specimens is typically the result of physical phenomena known as luminescence, which occurs at electronically excited states. Luminescence is formally divided into two categories: fluorescence and phosphorescence, depending on the nature of the excited state. Fluorescence occurs when a photon excites an electron from the ground-state to a higher energy state, and the electron in the excited orbital is paired (of opposite spin) to the second electron in the ground-state orbital. Return to the ground state is spin allowed and occurs rapidly by emission of a photon producing fluorescence. The emission rate of fluorescence (fluorescence lifetime) is of the order of nanoseconds to microseconds. The lifetime τ of a fluorophore (fluorescence substance) is the average time between its excitation and its return to the ground state. Phosphorescence is the light emission from excited states, in which the electron in the excited orbital has the same spin orientation as the ground-state electron. Transitions to the ground state are forbidden and the emission rates are slow, in the order of millisecond to seconds (Lakowicz, 1991), (Lakowicz, 1999), (Gore, 2000), (Valeur, 2002).

The processes which occur between the absorption and emission of light are usually illustrated by a Jablonski diagram (figure 1). S0, S1 and S2 denote ground, first, and second electronic states. At each of these electronic energy levels the electrons can exist in a number of vibration energy levels denoted by 0, 1, 2, etc. The transitions between states are depicted as vertical lines to illustrate the instantaneous nature of light absorption (10^{-15}s). An electron is usually excited to some higher vibration level of either S1 or S2 and rapidly relaxes (10^{-12} s–10^{-15} s) to the lowest vibration level of S1. Return from level S1 to the ground state S0 produces fluorescence emission. Examination of the Jablonski diagram revels that the energy of emission is less than that of absorption. Hence, fluorescence occurs at lower energies or longer wavelength (Stokes shift). The amount of Stokes shift is a measure of the relaxation process occurring in the excited state, populated by absorption. Another property of fluorescence is that the same fluorescence emission spectrum is generally observed irrespective of the excitation wavelength. This is known as Kasha´s rule. Although fluorescence measurements are more sophisticated than an absorption (transmission) experiment, they provide a wealth of the information about the molecular structure, interaction and dynamics of species.
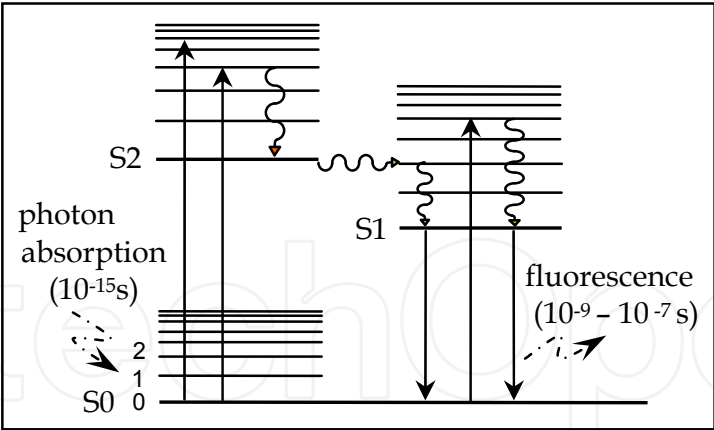
Fig. 1. A simple Jablonski diagram

Two important characteristics of a fluorophore are its quantum yield and its fluorescence lifetime. The quantum yield is the number of emitted photons relative to the number of absorbed photons, and it is given by equation (1). Γ is the decay rate by spontaneous emission and knr is the decay rate which do not produce radiation, and it is associated to energy losses by vibrational relaxations and internal conversions. The fluorescence lifetime τ is defined as the average time from the fluorophore excitation to the return to ground state, when the optical excitation is a δ impulse function and it can be expressed as (2).

$$Q = \frac{\Gamma}{\Gamma + knr} \tag{1}$$

$$\tau = \frac{1}{\Gamma + knr} \tag{2}$$

The population in excited state decays at rate $\Gamma + knr$ according to equation (3), where n(t) is the number of excited molecule. In fluorescence spectroscopy, instead of excited molecule n(t), an equivalent quantity as irradiance I(t) is measured. The result is an exponential decay of the irradiance as equation (4). The lifetime τ is the decay time from maximum value Io to its fraction 1/e.

$$\frac{dn(t)}{dt} = \frac{1}{\tau} n(t) \tag{3}$$

$$I(t) = Io \, \exp(-t / \tau) \tag{4}$$

1.2 Fluorescence measurements

Fluorescence measurements can be broadly classified into two types: steady-state and time-resolved. Steady-state measurements are those performed with constant illumination and observation, this is the most common type of measurement. The sample is illuminated with a continuous beam of light and the intensity of the emission is usually recorded as a wavelength function (fluorescence spectrum), as it is shown in figure 2. When the sample is exposed to light, steady state is reached almost immediately. Time-resolved measurements are used for measuring intensity decays. For those measurements, the sample is exposed to a pulse of light, where the pulse width is typically shorter than the decay time of the sample.

The intensity decay is recorded with a high speed detection system that allows the intensity to be measured on a nanoseconds timescale. Figure 3 shows an example of time-domain measurement of an excitation laser pulse and the fluorescent response pulse. Time-dependent measurements resolve fluorescence intensity decays in terms of lifetimes, and thus provide additional information about the intra and intermolecular dynamics of the fluorophore (the fluorescent compound of the sample) under study (Lakowicz, 1991), (Lakowics, 1999), (Gore, 2000).
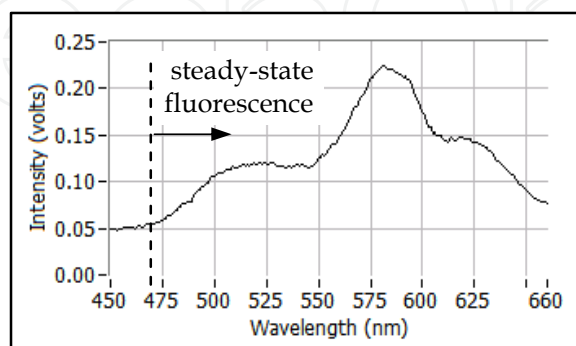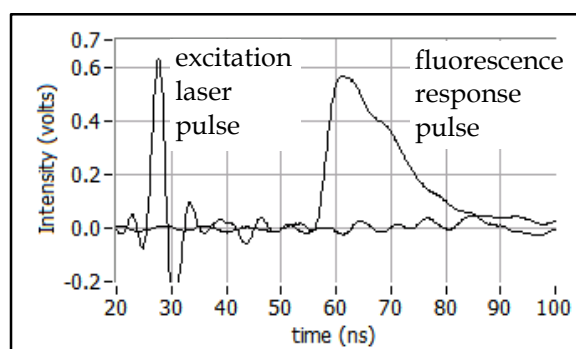
Fig. 2. Steady-state measurements

Fig. 3. Time-resolved measurements

There exists a rather simple relationship between steady-state and time-resolved measurements. The steady-state intensity Iss is an average of the time resolved phenomena over the intensity decay of the sample, as equation (5). The value of the intensity Io depends on the fluorophore concentration.

$$Iss = \int_0^\infty Ioe^{-t/\tau}dt = Io\tau \tag{5}$$

Figure 4 shows the general structure of a spectrofluorometer to measure steady-state and time-resolved fluorescence. Usually, the sample under study is excited with ultraviolet light, the sample emits florescence in all directions, and part of this emission is captured at the monochromator input. The monochromator output is a light with a single wavelength (λ) component of the input light, coming from the sample. The light from the monochromator output is captured by a photodetector (FD), which produces a current signal proportional to response fluorescence signal. This electrical signal is processed and acquired to be read by the computer.
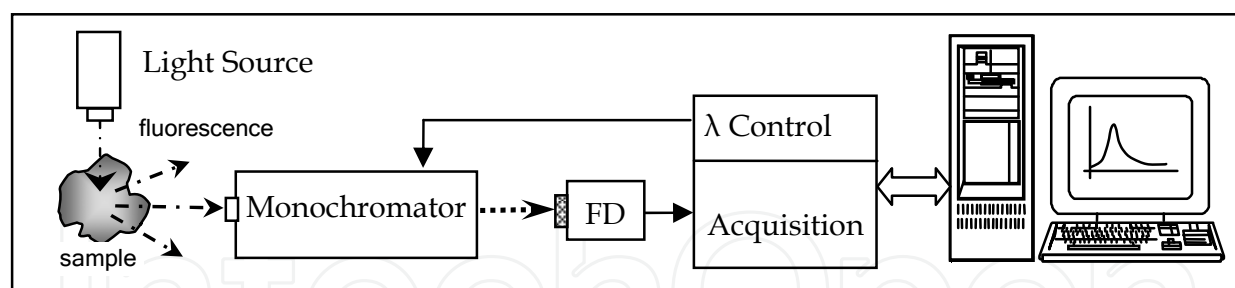
Fig. 4. General structure of a spectrofluorometer

The main differences between steady-state and time-resolved fluorometers are two: the light source (continuous or pulsed) and data acquisition process requirements. For steady-state measurements the values to acquire are constant, and thus there are not high speed requirements. The acquisition process uses real-time sampling technique. A low cost DAQ board or microcontroller is enough to acquire steady-state data. A time-domain fluorometer requires a high speed digitizer to resolve ns fluorescence decays. Normally this digitizer uses an equivalent-time sampling method to acquire temporal data on nanoseconds timescales. It is a common practice to use a digital oscilloscope as digitizer system.

1.3 Fluorescence applications

The spectrofluorometry is related to the measurement of the emission spectra produced by fluorescent samples, it is the most extensively used optical spectroscopic method in analytical measurements and scientific investigation to measure the concentration species in gases, liquids and solids. In the scientific research laboratory, fluorescence spectroscopy is being used or applied to study the fundamental physical processes of molecules, structure-function relationships and interactions of biomolecules (Gore, 2000), (Valeur, 2002). In-situ fluorescence measurements are too very important in others areas as the study of water and soil contamination (Anderson et al., 2003), the chlorophyll fluorescence in green plants to know their physiological and health status (Nesterenko et al., 2007), the study of chemical and physical changes in dairy products caused by processing and storage (Moller & Mortensen, 2008), or for adulteration assessment (Poulli et al., 2007).

The fluorescence spectroscopy is now widely used for biomedical purposes and clinical analysis. The fluorescence emission from the skin can be used to monitor changes induced by the UV radiation. *In vivo* spectrofluorometry has emerged as a powerful technique for biomedical research covering abroad spectrum, from study of cellular and tissue structures, to biological function and early detection of cancer (Paras, 2003), (Tuan, 2003). Optical biopsy refers to detection of cancerous state of a tissue using optical methods. This is a new area, offering the potential to use noninvasive or minimally invasive *in vivo* optical spectroscopic methods, to identify a cancer at its various early stages and monitor its progression. The basic principle utilized for the method of optical biopsy is that the emission fluorescence is strongly influenced by the composition and the cellular structures of tissues. The changes in tissue from normal state to cancerous state have been show to alter the fluorescence. Biomedical fluorescence spectroscopy is an extremely large and growing field of research (Paras, 2003), (Tuan, 2003).

2. Time-resolved fluorescence spectrometer

Figure 5 shows the experimental arrangement of a home made instrument to measure time-resolved fluorescence signals emitted by samples under study. The nitrogen laser (N_2) generates short light pulses to a beam divider, where part of the incident light is reflected toward a reference photodiode (PD). This detector produces an electric pulse, similar to laser pulse, which triggers the oscilloscope to start an acquisition process of the signals present on both oscilloscope input channels. Most of the laser pulse passes trough the divider to an optical chamber formed by a biconvex lens, an ultraviolet filter (337.1 nm) and a sample holder.
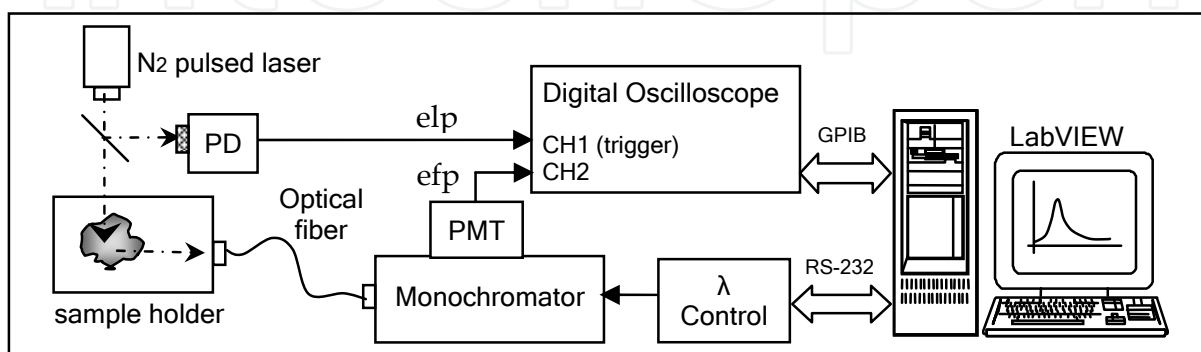

Fig. 5. Time-resolved fluorescence spectrometer

The response fluorescence pulse emitted by the sample is collected by an optical fiber and delivered to monochromator input. The luminous pulse at monochromator output is detected by a photo multiplier tube (PMT) and converted to an electrical current pulse. The laser (elp) and fluorescence (efp) electrical pulses are measured with oscilloscope channels 1 and 2, and the information registered of both signals is sent to a computer via a GPIB interface. These time-resolved signals correspond to a single monochromator output wavelength. The wavelength control communicates with the computer via a serial port RS-232. A control program was developed in the graphical language G of LabVIEW™ 7.1 to control the process, and to register and plot the time-resolved pulses.

2.1 Pulsed light source

When a fluorophore is excited with light, the emitted fluorescence propagates in all directions, and only a small fraction of fluorescence intensity reaches the monochromator input. Therefore a light source with relative high power emission is required. It has been common practice to use a nitrogen laser, as monochromatic pulsed light source in fluorescence spectroscopy. Now days the nitrogen laser can be replaced by a laser diode but at a higher cost. During the past years the light emitter semiconductor materials have been improved, lowering wavelengths up to deep UV region, and increasing emission powers, at lower costs than laser diodes (Geddes & Lakowicz, 2004). Figure 6 shows a home made nitrogen laser system. The nitrogen is injected to a discharge chamber at around 20 mbar. When the spark-gap (SP) is open the capacitors C_1 and C_2 are charging from the high dc voltage supply and a 10 MΩ resistors bank (inductance L behaves as short-circuit). The voltage trough capacitors increases exponentially up to the spark-gap threshold voltage, then C_1 discharges immediately trough the spark-gap, and C_2 discharges trough the nitrogen inside the chamber (now L behaves as open-circuit). The excited nitrogen by the

discharge produces an ultraviolet light pulse (337. 1 nm) at chamber output. After discharge the spark-gap is open, L behaves as a short-circuit, and capacitors voltage start to increase again. The repetition rate of laser pulses is given by time constant RC (around 30 ms) and the applied high voltage. With 10KV a frequency rate near 30 Hz is obtained.
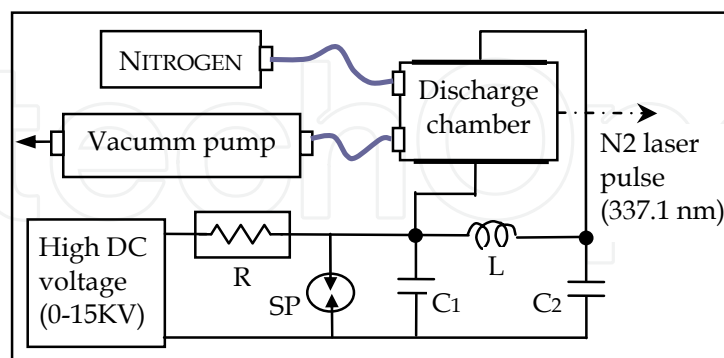
Fig. 6. Nitrogen pulsed laser

2.2 Monochromator

A monochromator is an optical system which decomposes an input light in its different wavelength components, and selects a single wavelength component at its output. Most of monochromators used in fluorescence spectroscopy contains a diffraction grating as dispersion element, since the inverse of the dispersion factor (D^{-1}) is constant at all wavelength. This parameter has nm/mm units and relates the effective wavelength bandwidth which goes trough the monochromator input slit, it is a quality factor of the monochromator (typical values: 2–8 nm/mm). The wavelength resolution is not important since the fluorescent emission spectra are wider than 5 nm. Normally, monochromators have input and output adjustable slits. The luminous intensity at any slit input is approximately proportional to the square of the slit width. For wider slits more light goes through the slit and then, the signal to noise ratio increases. A narrow slit improves the resolution at intensity expenses (Lakowicz, 1991), (Lakowics, 1999), (Gore, 2000).

For our spectrofluorometer we use a monochromator from Acton Research Corp., model SpectraPro 275, which is of the Czerny-Turner type with focal length of 275 mm. The instrument contains three selectable gratings for three different wavelength intervals. We use a grating with 2400 groves/mm for a 200 - 750 nm interval. The reciprocal linear dispersion factor D^{-1} is 3 nm/mm. The equipment includes a microprocessor control with menu driven software for scan control, grating selection, and change of scanning speed. All scanning functions and control parameters are selected locally from a keypad and a LCD display. Computer control is provided trough a standard RS-232 port.

2.3 Photodetectors

Perhaps the most used photodetector for time-resolved fluorescence spectroscopy is the photomultiplier tube (PMT), because two relevant characteristics: its high gain with low noise, which allows detecting weak fluorescence signals, and its fast response. A PMT consists of a photocathode covered with an emitter surface and a chain of electrodes (dynodes) which acts as amplification stages. The photocathode is supplied with a high negative potential (-1 KV to -2 KV) and dynodes also are supplied with negative potentials,

but less in magnitude for each dynode in the chain. The radiation reaching the photocatode produces emission of some primary electrons which are accelerated to the first dynode. When each one of these electrons hits the dynode several additionally electrons are emitted by collisions, and accelerated to the next dynode. The amplification process is repeated successively and the produced current is collected at the end of the chain (Lakowicz, 1999).

Other photodetector of growing use in steady-state fluorescence spectroscopy is the charge coupled device (CCD). This device consists of a thin silicon substrate with thousands or millions of small photodetectors elements, in one or two dimensional array. The substrate is coupled to metallic electrodes by means of silicon dioxide, and each element of the array functions as a MOS photodiode and capacitor (storage element). The charge related to the light intensity detected by each image element (pixel), is acquired sequentially and then converted into a digital format inside de same CCD (Spring, 2010).

An instrument with a single channel photodetecor like a PMT, produces a spectrum by means of the diffraction grating. For each grating position, a single point of information is registered. In contrast, a multichannel detector like CCD collects many points simultaneously; this permits to acquire a complete spectrum data in a single exposition. The acquisition speed of steady-state spectrum is much higher with a CCD (almost real time), compared with the acquisition speed with PMT (point by point). The major disadvantage of a CDD is its slow response time, or limited bandwidth, and then its application in time resolved spectroscopy is limited.

Now days there are complete PMT modules which include: a cd-cd converter to supply the high voltage required by the PMT, from a single +15 V supply, a cd voltage input to control PMT gain, and an output reference voltage. We use the PMT module H7732P-11 manufactured by Hamamatsu. This module contains a high sensitivity photomultiplier tube with 4x20 mm² of effective area of detection, a peak radiant sensitivity of 80 mA/W at 430 nm, 2 ns characteristic rise-time, and a capacitance of 4 pF. The output current pulse generated by the PMT is sent the oscilloscope through a coaxial cable. A voltage pulse is produced through the input impedance of the oscilloscope analog input. This impedance must be low enough to increase the bandwidth at the analog front end of the oscilloscope (see section 2.4)

In figure 5 a fraction of the laser pulse is reflected by a beam divider toward a reference photodiode. When the photodiode is negative biased, it produces an inverse current proportional to the light intensity, detected by its active area at the junction. The photodiode produces a current pulse similar to laser pulse which excites the sample. Also this reference current pulse is converted to a voltage pulse trough the input impedance of the oscilloscope analog input. This reference pulse is used as trigger signal to the oscilloscope to start the acquisition process on both input channels. We use the fast photodiode MRD500 with a response time of 1 ns on 50 Ω load, a sensitivity of 1 nA/mW/cm2 at 337.1 nm, and a capacitance of 4 pF.

2.4 Time-domain measurements

An automatic process for time-domain measurements involves the use of a digitizer (programmable digital system or digital oscilloscope), thus the continuous-time fluorescence pulse to measure has to be converted to a digital format in order to be recognized by the digital system. There are two basic sampling methods to perform the analog-to-digital conversion (ADC): real-time sampling and equivalent-time sampling. Equivalent-time sampling can by dived further into two sub-categories: random and sequential. Each

method has distinct advantages depending on the kind of measurements being made (Lawton, 1986), (Nahman, 1978). Real-time methods require only a single occurrence of the signal to acquire an entire waveform, and the sampler operates at maximum speed to acquire as many points as possible in one sweep. Figure 7 shows the real-time sampling process with a sample rate = $1/Ts$.

Equivalent-time methods, on other hand, require multiple occurrences of the signal to acquire the waveform. Samples are acquired over many repetitions of the signal, with one or more samples taken on each repetition. The sequential equivalent-time technique includes a trigger signal as figure 8 shows.
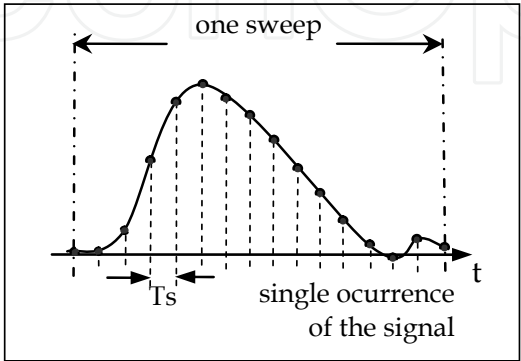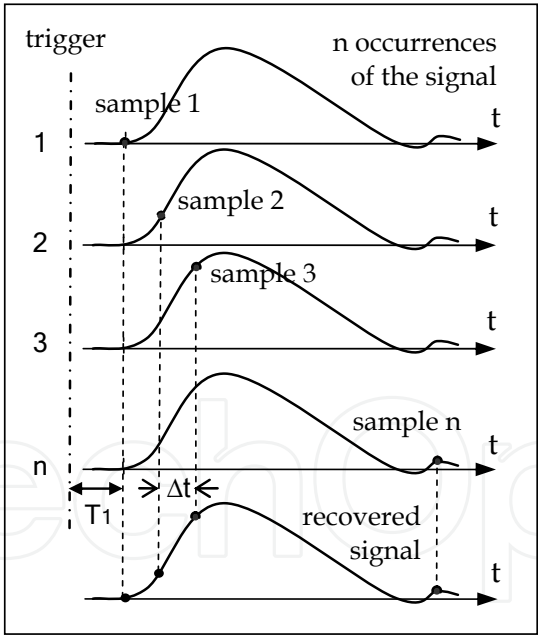

Fig. 7. Real-time sampling

Fig. 8. Sequential equivalent-time sampling

When the first trigger is detected the first sample is taken after a fixed initial time T_1. At the next period, a second sample is taken after a very short, but well defined, delay Δt from the time position of the first sample. When the next trigger occurs, the same time Δt is added to the previous delay and another sample is taken. This process is repeated many times, and after n periods of the signal, n samples have been taken to recover the waveform of the signal. If the sample point is shifted in sufficiently small steps Δt, this sampling method provides a very high bandwidths (65 GHz and higher) and timing resolution needed for

time-resolved fluorescence signals. In random equivalent-time mode, portions of waveforms are acquired in real-time sampling during multiple trigger events. Over time, these portions are assembled into a complete waveform. Modern digital programmable oscilloscopes apply the three sampling techniques mentioned before, depending on the kind of measurements being made. In fluorescence spectroscopy, where nanoseconds times have to be resolved, the sequential equivalent-time is normally used.

To measure the reference and response signals in figure 5, we use the digital oscilloscope model 2440 from Tektronix®. This oscilloscope has 300 MHz analog input bandwidth, 500 MS/s maximum sampling rate, and 1 MΩ input impedance. This impedance can be programmed to be 50 Ω, as it is needed to measure the current signals coming from the photodetectors. Most of the oscilloscope features can be programmed from its rear panel, or from a computer via its GPIB port. We use the interface board GPIB-USB-HS from National Instruments, which is directly connected to the oscilloscope GPIB port. This board communicates with the computer via USB interface.

2.5 Bandwidth and rise-time specifications

Particularly we are interesting to time-resolve fluorescence lifetimes in nanoseconds order. For these very short times there are two important specifications of the acquisition system behavior to consider, these are its bandwidth analog front end BW(afe) and its equivalent rise time tr(afe). Bandwidth describes the analog front end's ability to capture an analog signal with minimal amplitude loss, and rise time slowing. Bandwidth is defined as the frequency at which the amplitude of the sampled signal decays 30% due to ADC performance. The rise time for a signal is defined as the time to transit from 10% to 90% of the maximum signal amplitude. Both concepts can be applied in general to signals, to systems, or to components, and they are inversely related by equation (6), which is based on the one pole model, R-C limited input response [Ardizzoni, 2007].

$$\mathrm{BW} = \frac{0.35}{\mathrm{tr}} \qquad (6)$$

In our instrument the rise-time at analog front ends of the oscilloscope can be estimated from the time constant introduced by photodetectors output capacitance, and the impedance of the oscilloscope input channels. The rise-time for this RC circuit is given by tr = 2.2RC, where the input impedance R must be low enough to decrees rise-time (or to increase the bandwidth) at analog front end. The capacitance has a value of 4 pF for both photodetectors, and the input impedance is programmed to be 50 Ω, thus the rise-time at analog front end of both input channels is 0.44 ns or equivalently 800 MHz bandwidth according to equation (6). Not only the rise-time of the analog front end at acquisition system input, but also rise-times of oscilloscope and photodetectors contribute to slowing the input signal. The measured rise time tr(m) can be estimated by using a sum-of-squares technique as equation (7), where tr(exc) is the excitation pulse rise-time, and tr(eq) is the equipment characteristic rise-time (Weller, 2002). The equipment square rise-time can be expressed as equation (8), where each term in summation is the square rise-time of the k component in the measuring chain.

$$\mathrm{tr}^2(\mathrm{m}) = \mathrm{tr}^2(\mathrm{exc}) + \mathrm{tr}^2(\mathrm{eq}) \qquad (7)$$

$$\mathrm{tr}^2(\mathrm{eq}) = \sum_{\mathrm{k}} \mathrm{tr}^2(\mathrm{k}) \qquad (8)$$

Figure 9 shows a diagram with the main components in our electronic instrumental, where rise-times and bandwidths values are indicated for each component. Some of these values are given by manufacturers and others are calculated from equation (6).
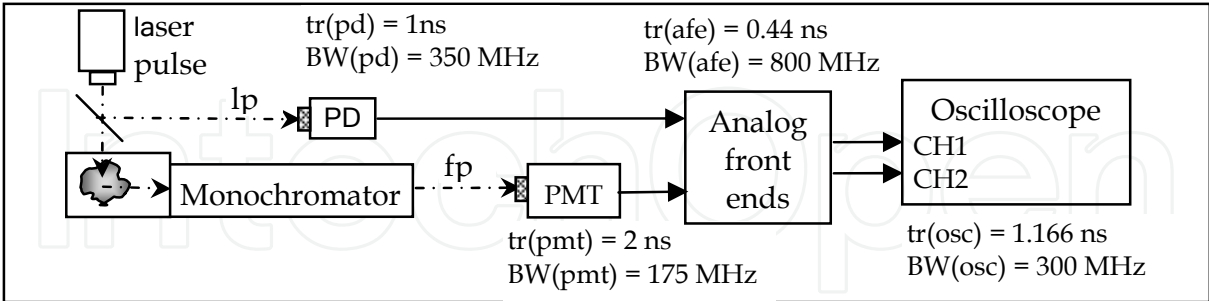

Fig. 9. Characteristic rise-times and bandwidths of each component of the measure chain

The laser pulse (lp) is detected by the photodiode (PD) and the fluorescence response pulse (fp) is detected by the PMT. From values in figure 9 and equation (8) we calculate for PD: $tr(eq)_{PD}$ = 1.59 ns, and for PMT: $tr(eq)_{PMT}$ = 2.35 ns. The laser pulse measured by the oscilloscope (figure 19, section 3.3) has a rise-time $tr(lpm)$ = 1.78 ns, thus we can estimate the rise-time of the laser pulse as follows:

$$tr(lp) = \left(tr^2(lpm) - tr^2(eq)_{PD}\right)^{1/2} = 0.821\,ns \tag{9}$$

If the sample does not emit fluorescence (distillated water, per example) the laser pulse enters directly to monochromator, and then the measured signal corresponds to the system response and we can write the following expression:

$$tr^2(spm) = tr^2(lp) + tr^2(eq)_{MC\text{ - }PMT} \tag{10}$$

where $tr(srm)$ is the rise-time of the system response pulse measured by the oscilloscope (figure 19) with a value of 5.64 ns, and $tr(eq)_{MC\text{-}PMT}$ is the equipment rise-time including monochromator rise-time. From values obtained we can assume $tr^2(srm) >> tr^2(lp)$, and then $tr(eq)_{MC\text{-}PMT}$ is approximately equal to $tr(srm)$. This is the characteristic rise-time which slowing the fluorescence response signal, and it is mainly caused by the monochromator rise-time, for which we estimate $tr(mc)$ = 5.13 ns. Other used form to quantified the slowing of the input signal is by means of the system temporal resolution, which is expressed in terms of pulse widths Δt as equation (11) (Lakowicz, 1991).

$$\Delta t^2(m) = \Delta t^2(exc) + \Delta t^2(eq) \tag{11}$$

3. Spectrofluorometer control program in LabView

A control program was developed in the graphical language G of LabVIEW 7.1 environment. This program controls the monochromator to generate a wavelength (λ) sweep, and reads the information of the time-resolved signals (excitation and response) measured by the oscilloscope in each λ value. The program was designed to execute one of three main functions, these are: a) *GoTo/Measure Noise*, b) *Sweep*, and c) *Open Files*. Following lines describe the algorithm for the main program.

S0) Serial Port Init.vi, goto λ.vi (250nm), actualλ = 250 nm   ; initiation, sequenceS0
S1) while (STOP=false)   ; sequence S1
    case (Tab Control)
        Go To / Measure Noise   ; wait for a sub function <u>Go to λ</u> or <u>Measure Noise</u> = on
        Sweep   ; wait for a sub function <u>Start</u> = on
        Open Files   ; wait for a sub function <u>Time Domain</u> or <u>Spectrum</u> = on

In sequence S0, the serial port is initialized and the monochromator is positioned at 250 nm output wavelength, by means of the subvi "goto λ.vi". Then in sequence S1) a while sentence is executed for ever up to "STOP" control on the front panel (figure 16) is pressed. The function to execute is selected by means of a "Tab Control", for each function the panel shows the proper controls to start a sub function execution. Before reviewing the objects on the front panel we describe the program functions and developed subVI´s. Figure 10 shows a simplified diagram of the control logic during initial while sentence, when function *Go To/Measure Noise* is selected. For this function there are two sub function controls: if <u>Measure Noise</u>=on (as in figure 10) the respective algorithm is executed, if <u>Measure Noise</u>=off, means <u>Go to λ</u>=on, and then in the inner case structure, the "False" sentence executes the correspondence algorithm.
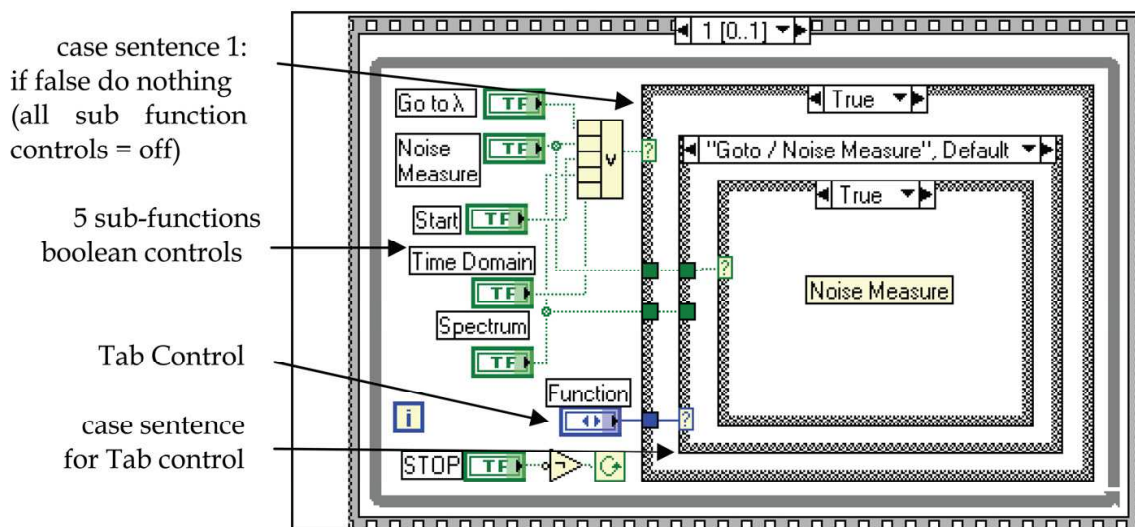

Fig. 10. Main while sentence S1

3.1 Functions and SubVi´s
Following lines describe the algorithms of program functions and developed subVI´s. Some LabVIEW diagrams are included.

a) Go To/Measure Noise
    wait for (<u>Go To λ</u> or <u>Measure Noise</u> = on)
    if <u>Go To λ</u>=on ; see diagram in figure 11
        VER. Interval.vi   ; verify valid values of λ, if not valid, do nothing and display an
            error message
        goto λ.vi (λ to go) ; sends a command via serial port to move the monochromator
            from the actual value of λ (actualλ) to the destination value of λ (λ to go)
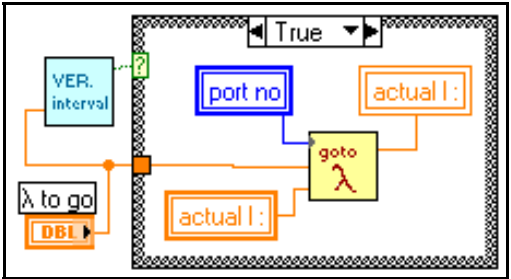   actualλ = λ to go

Fig. 11. Sub function <u>Go To λ</u> = on

    if <u>Measure Noise</u> = on ; see diagram in figure 12

        TM2440.vi (CH1, CH2, XInc) ; this sub.vi controls the oscilloscope via GPIB interface, to start a waveform acquisition of signals at channels 1 and 2. Acquisition ends when the oscilloscope had measured 16 waveforms of both input channels. The oscilloscope calculates average values of the waveforms measured, and send the averaged signals to subVi outputs CH1 and CH2, as k length arrays with k=1024 (fixed by oscilloscope). The output X inc corresponds to time interval used by oscilloscope during its temporal sweep. This subVi is a reduced and modified version from the original LabVIEW driver for the used oscilloscope.

    noise1(k) = CH1

    noise2(k) = CH2

    time(k) = k*XInc

    graph noise1(k) and noise2(k) vs time(k) in XY Graph "noise"

    save data?

        if yes "Write to Spreadsheet. vi"

The contents of arrays noise1(k) and noise2(k) are interpreted as noise information to be subtracted dynamically from the measured signals during the sweep function.
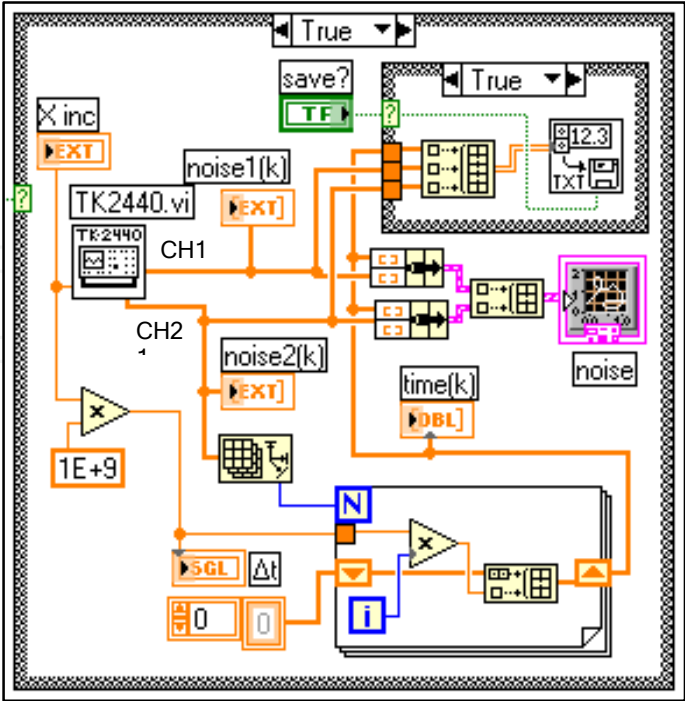

Fig. 12. Sub function <u>Measure Noise</u> = on

b) Sweep

    wait for (<u>Start</u> =on)

    VER. Interval.vi   ; verify valid λ values

    goto λ.vi (initialλ)   ; move monochromator from actualλ to initialλ

    actualλ = initialλ

    while (finalλ > actualλ)   ; sweep while

        TM2440.vi (CH1, CH2, XInc)

        lp(k) = CH1-noise1(k)   ;laser pulse measurement with noise subtraction

        fp(k) = CH2-noise2(k)   ;fluorescence pulse measurement with noise subtraction

        time(k) = k*XInc

        graph lp(k) and fp(k) vs time(k) in XY Graph "temporal response"

        nfp = max[fp(k)]/max[lp(k)]; because de laser pulse amplitude is not constant, it is
                                 necessary to normalize the fluorescence pulse
                                 amplitude at maximum peak

    save in file: time(k), lp(k), fp(k)

        Figure 13 shows a sequence where the file with the time-domain information is saved at locations given by the Path control and a string. This string is formed with the Base Name control and the value of actualλ, thus the file name contains the wavelength value at which the temporal data were measured. In the diagram there is a boolean constant to avoid saving time-domain data during the test procedures.

    add element actualλ to array λ(j), and element nfp to array nfp(j)   ; see figure 13

    graph nfp(j) vs λ (j) in XY graph "spectrum"   ; see figure 13

    goto λ.vi (λactualλ + Δ λ)

    actualλ = actualλ + Δ λ

  save spectrum λ(j), nfp(j) ?; when sweep loop ends the complete spectrum can be saved
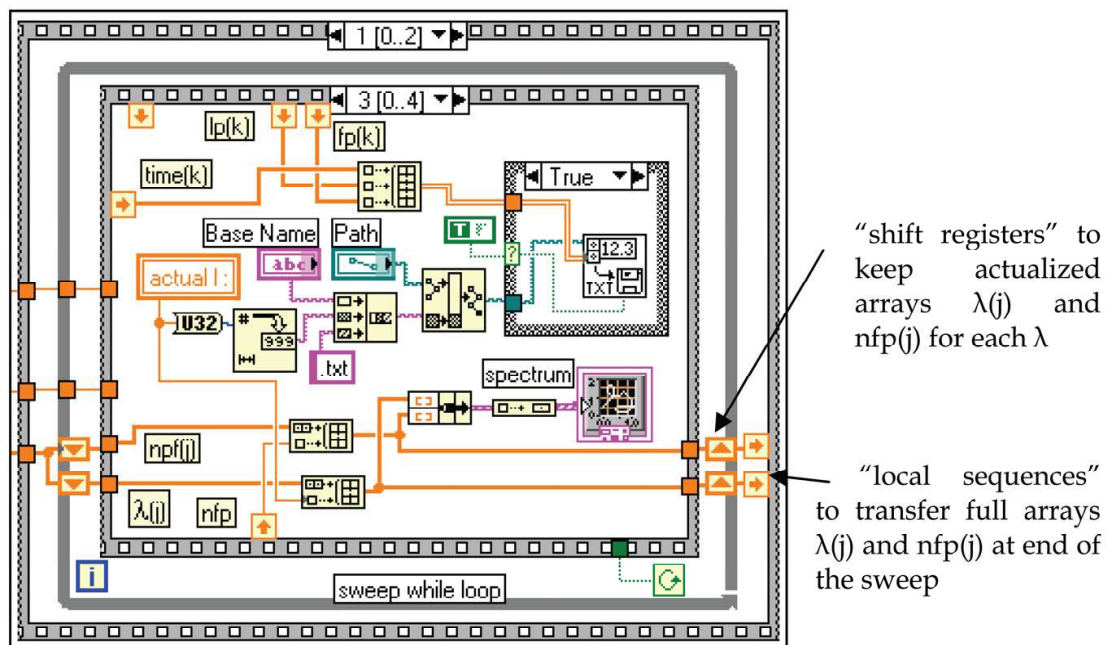

Fig. 13. A sequence of *Sweep* function to save time-domain data measured in a file with a name containing actual λ value

c) Open Files

wait for (Time Domain=on or Spectrum=on)

if Time Domain =on

open temps.vi   ; this subVi can open several files with time-domain data and graph these in its own XY Graph. Each time that a new file is opened the graph is actualized. Because the subVi keeps in loop waiting for a new file to open, the information of this graph is transferred to the main panel XY Grap called "tempResponses", by means of "control references", as figure 14 shows.

if Spectrum=on

open spectra.vi ; this subVi performs similar to the previous one, but it opens spectra data. Also uses "control references"

SubVi: goto λ.vi (λ to go)
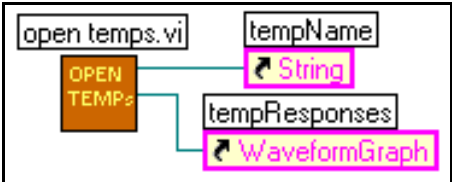
Fig. 14. "control references"

Figure 15 shows the two first sequences of subVi goto λ.vi. At left in first sequence, a string is ensemble to form the command "goto" recognized by the monochromator control. The command is sent to control via Serial Port Write.vi. Once the monochromator motor starts to move, it takes a time to reach the value of λ to go from actual λ. In second sequence this time is calculated according to maximum speed, and it is used as input to a delay element. It is important to reach λ to go before the oscilloscope starts an acquisition process.
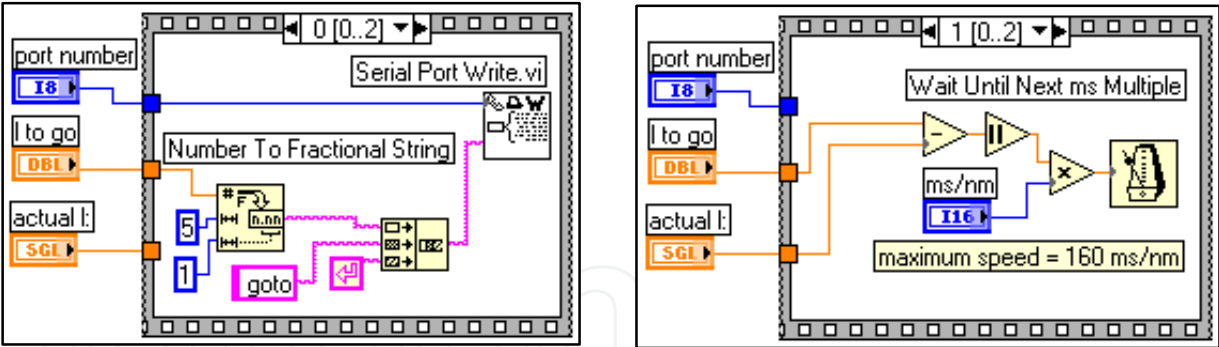

Fig. 15. First two sequences of SubVi goto λ.vi λ to go).

3.2 Front panel

The front panel of the developed program is shown in figure 16, where *Sweep* Function is selected by a Tap Control. At left there are 3 numeric controls to introduce λ values of the sweep to perform. At top there are two controls to introduce the Path and Base Name of the files to store time-domain information for a complete sweep. With selected values, the *Start* control is pressed to begin the sweep. First the monochromator output wavelength is controlled to move from actual λ (indicator at top-left corner on the panel) to initial λ, and then the oscilloscope is controlled to start waveform acquisition of laser pulse and fluorescence pulse. Each recorded laser and fluorescence pulses consisted on average

Fig. 16. Frontal Panel when *Sweep* function is selected and stopped at 560nm.

of 16 consecutive pulses computed by the oscilloscope before transfer to the computer. After receiving time-domain data from oscilloscope, the computer graphs the average time-resolved pulses on "temporal response" graph in figure 16, calculates the normalized peak fluorescence, and graphs this value on "spectrum" graph. The computer shifts the monochromator output wavelength by 5 nm and reset the oscilloscope for the next measurement. The sweep loop ends when final λ value is reached or Stop control is pressed (bottom-left corner). In figure 16 de sweep was stopped by "Stop" control, when monochromator was moving from 560nm to 565nm. The panels for other two functions show only their respective controls and indicators, similar to those in figure 16.

3.3 Measurements

Using the described spectrofluorometer and LabView program, we measured the fluorescence emitted by 3 substances with well known fluorescence life-times; these are fluoresceine, rhodamine 6G and rhodamine B. Their properties vary according to the used solvent. For distillated water as solvent, the life-time and wavelength at maximum emission of the fluorophores are: fluoresceine (4.03 ns, 517 nm), rhodamine 6G (4.08 ns, 555 nm) and rhodamine B (1.68 ns, 583 nm). Also we measured the fluorescence emitted by 3 mixtures of two fluorophores. For each fluorophore and mixture, were performed 6 wavelength sweeps

from 400nm to 700nm with 5nm increments. The average spectra obtained for individual fluorophores are shown in figure 17, where λ value at maximum emission is indicated for each substance. Figure 18 shows the average spectra obtained for 3 mixtures of two components (50% each): fluoresceine–rhodamine 6G (f-r6G), fluoresceine–rhodamine B (f-rB) and rhodamine 6G–rhodamine B (r6G-rB).
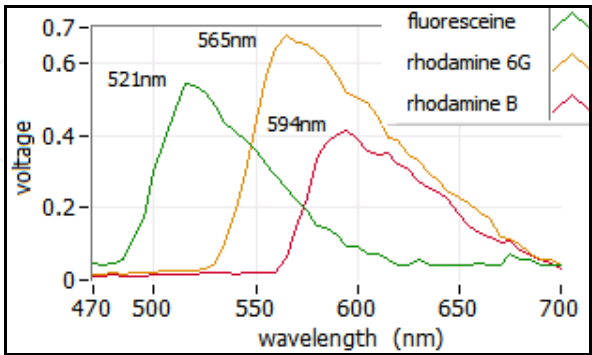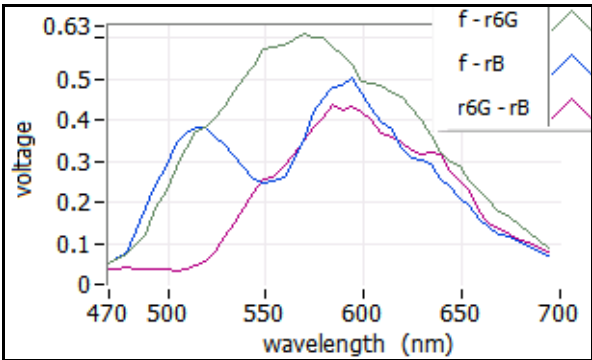

Fig. 17. Average spectra of fluorophores

Fig. 18. Average spectra of mixtures

In figure 17 we observe that wavelengths at maximum emission peaks of the three fluorophores, are greater than the before mentioned reference values. These deviations may be produced because monochromator is out of calibration. In figure 18 the spectrum of mixture f-rB shows the emission peaks, one around 521 nm and other near 594 nm, both fluorophores. Because the spectra of the fluoresceine and the rhodamine 6G, and the spectra of the rhodamine 6G and the rhodamine B, overlap each other in a wider region. The wavelength at maximal emission in both mixtures are shifted in relation to their pure components.

Figure 19 shows the average time-resolved laser pulse and the system response pulse. This pulse was measured using distillated water as sample, which does not produce fluorescence. From recorded data we estimate for laser pulse tr(lpm) = 1.78 ns and FWHM(lpm) = 2.752 ns, and for system response pulse tr(srm) = 5.647 ns and FWHM(srm) = 13.28 ns. The average time-resolved fluorescence responses, measured for each fluorophore are shown in figure 20, where corresponding λ value is indicated. Figure 21 shows the average time-resolved fluorescence responses measured for each mixture at two different wavelengths. In section 4 we apply an analysis technique to estimate fluorescence life-times from the measured data.
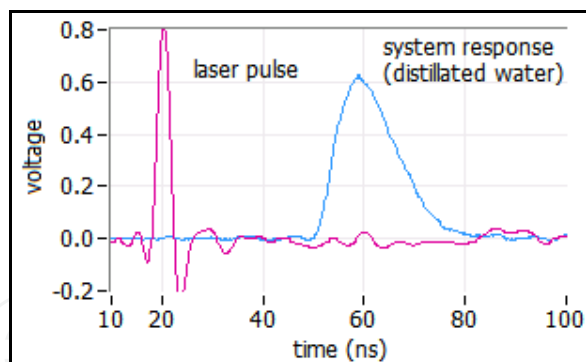
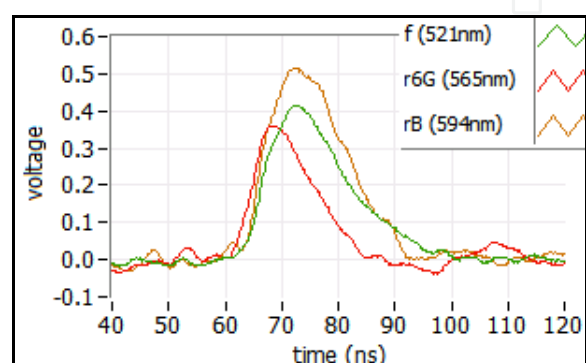Fig. 19. Average time-resolved laser pulse and system response pulse

Fig. 20. Average time-resolved fluorescence responses each fluorophore
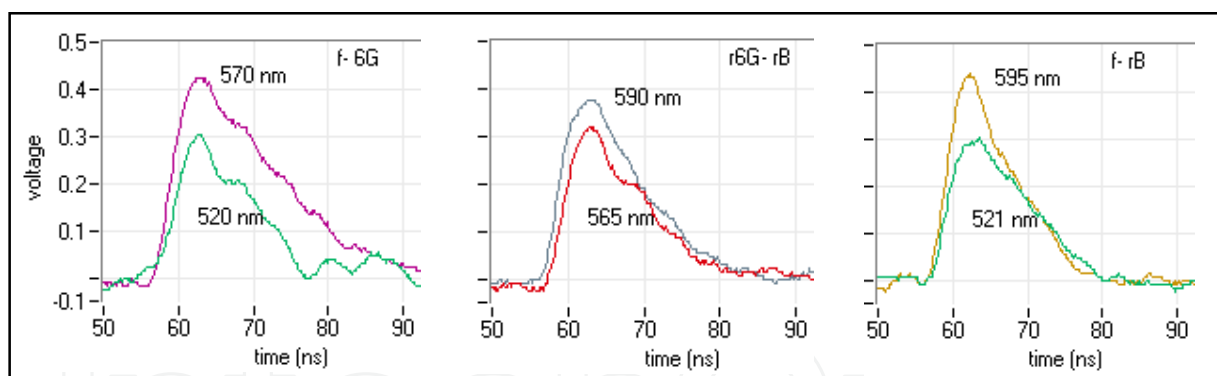

Fig. 21. Average time-resolved fluorescence responses of mixtures

4. Data analysis to estimate fluorescence lifetimes

In section 1.1 we stated that the fluorescence intensity due to a population of excited-state molecules decreases exponentially with time, following their instantaneous optical excitation, but equation (4) is only valid for δ impulse optical excitation. In practical time-domain spectroscopy, the excitation light pulse is of finite duration, and can be consider a δ function only if the florescence exponential decay is much greater than the excitation light pulse width. On other hand, there is not a direct relation between the exponential model of equation (4) with measured decays, meanly because the measurement instrumental introduces amplitude loss and rise time slowing of the signals to measure (section 2.5). Thus it is necessary to apply data analysis techniques to find the best estimation of fluorescence lifetimes.

4.1 Convolution integral and instrumental response

Mathematically, the fluorescence intensity decay data y(t) of a sample excited by a short pulse of light, is given by the convolution of the impulse response function h(t) (also called IRF) of the fluorescent sample, with the excitation light pulse f(t), i.e.

$$y(t) = h(t)*f(t) = \int_{-\infty}^{\infty} h(\tau)\, f(t\text{-}\tau)\, d\tau \qquad (12)$$

The impulse response function h(t), represents the undistorted decay law of the sample which we want to estimate. If the excitation is an ideal δ function, the observed fluorescence y(t) is equal to the impulse response. In practice, the excitation light pulse is not a δ function, and then this pulse must be deconvolved from observed fluorescence intensity pulse to obtain h(t) (Lakowicz, 1999). As we mentioned, the inclusion of the instrumental to measure the florescence emitted by the sample, introduces distortions in the measured signal. To consider this, the data acquisition process can be represented as figure 22, where f(t) represents the excitation optical pulse, h(t) represents the fluorescence decay of the sample, y(t) is a signal with fluorescence information, s(t) represents the spectrometer response, and m(t) is the signal measured. The convolution of the complete system is given by equation (13).

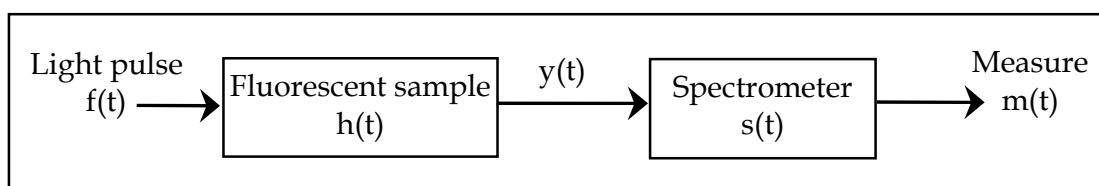Fig. 22. Inclusion of the spectrometer response s(t) to measure the y(t)

$$m(t) = s(t) * y(t) = s(t) *\ [h(t) * f(t)] \qquad (13)$$

To recover the fluorescence information from measured signals f(t) and m(t), the spectrometer response s(t) must be known. If the sample does not produce fluorescence (i.e. distillated water), thus h(t) = 1 and the measured signal represents the instrumental response: ir(t) = s(t)*f(t). Substituting this convolution in equation (13) yields:

$$m(t) = ir(t) * h(t) \qquad (14)$$

Then, to estimate the intrinsic fluorescence h(t), the measured fluorescence m(t) must be deconvolved from the measured instrumental response ir(t).

4.2 Deconvolution techniques

Several deconvolution techniques have been developed to estimate the intrinsic fluorescence decay h(t) of a sample, from measured signals m(t) and ir(t). The measurement of these signals involves an analog to digital conversion process, where the signals are sampled in discrete times t_n. To be according with mathematical variables, we renamed our measured variables: $y(t_n)$ represents the fluorescence measured, and $f(t_n)$ represents the instrumental response. For discrete time the convolution of equation (14) becomes a summation as equation (15), where N is de number of samples, and T is the sampling interval.

$$y(t_n) = T \sum_{m=0}^{N-1} h(t_m) f(t_m - t_n) \qquad (15)$$

As first approach we use the Fourier transform deconvolution method, which transforms the convolution in time-domain to a product in frequency-domain (O´Connor, 1979), i.e:

$$Y(\omega_n) = H(\omega_n) \ F(\omega_n) \qquad (16)$$

In frequency-domain the intrinsic fluorescence $H(\omega_n)$ is calculated by division, and then $h(t_n)$ is found by the inverse Fourier transform of $H(\omega_n)$. It is suggested the use of the fast Fourier transform to greatly reduce the inherent oscillations produced during the inverse transformation process (0´Connor, 1979). Data analysis of time-resolved fluorescence spectroscopy includes identification of a set of fitting parameters that best describe the characteristics of the fluorescence decay. Typically the intrinsic fluorescence $h(t_n)$ found by deconvolution is assumed to be a multiple exponential decays function, from where lifetimes τ are obtained.

Among other methods, the most commonly used deconvolution technique is the nonlinear least-squares iterative reconvolution (LSIR) method. This technique applies a least-squares minimization algorithm to compute the coefficients of a multiexponential expansion of the fluorescence decay. A variant of classical LSIR method assumes the intrinsic fluorescence $h(t)$ as an expansion on discrete time Laguerre functions, instead of a weighted sum of exponential functions (Maarek et all, 2000) (Jo et all, 2004). The Laguerre deconvolution technique uses an orthonormal set of discrete time Laguerre functions (LF) to expand the intrinsic fluorescence, i.e.:

$$h(t_n) = \sum_{j=0}^{L-1} c_j b_j^{\alpha}(t_n) \qquad (17)$$

where c_j are the unknown Laguerre expansion coefficients, which are to be estimated from input data; $b_j^{\alpha}(t_n)$ denotes the j´th order discrete time LF; and L is the number of LFs used to model $h(t_n)$. The LF basis is defined as equation (18), where the Laguerre parameter (0<*a*<1) determines the rate of exponential decline of the LF (Maarek et all, 2000) (Jo et all, 2004). Inserting equation (17) into equation (15), the convolution becomes as equation (19).

$$b_j^{\alpha}(t_n) = \alpha^{(n-1)/2}(1-\alpha)^{1/2} \sum_{k=0}^{j} (-1)^k n^k \binom{n}{k} \binom{j}{k} \alpha^{(j-k)}(1-\alpha)^k \qquad (18)$$

$$y(t_n) = \sum_{j=0}^{L-1} c_j \upsilon_j(t_n) \qquad (19)$$

$$\upsilon_j(t_n) = T \sum_{m=0}^{k-1} b_j^{\alpha}(t_m) f(t_n - t_m) \qquad (20)$$

In equation (20) $\upsilon_j(t_n)$ are the discrete time convolutions of the instrumental response with the LF. The unknown expansion coefficients can be estimated by generalized linear squares fitting of equation (19), using the measured discrete signals $y(t_n)$ and $f(t_n)$. This procedure involves the solution of a system of j equations. The optimal number of LFs and the value of the parameter α can be determined by minimizing the weighted sum of residuals:

$$\Phi = \sum_{n=0}^{N-1} w_n \left[y_0(t_n) - y_C(t_n) \right]^2 \tag{21}$$

where w_n is a weighting factor, $y_o(t_n)$ is the measured fluorescence, and $y_c(t_n)$ is the fluorescence computed by equation (15). Equation (15) is the convolution of the Laguerre expansion $h(t_n)$ of equation (17) with instrumental response $f(t_n)$. The iterative process ends when Φ reaches a minimum given value. The florescence decay lifetimes can by found by approximating the Laguerre expansion obtained to a multiexponential expansion.

4.3 Data analysis program

A data analysis program was developed in the graphical language G of LabVIEW 7.1 to estimate the intrinsic fluorescence decay $h(t_n)$, from deconvolution of the measured signals $y(t_n)$ and $f(t_n)$. This program applies the two deconvolution techniques described in section 4.2: Fast Fourier transform (FFT) and Laguerre expansion (LE). The intrinsic fluorescence $h(t_n)$ obtained with both methods is fitted to a simple exponential for a single fluorophore, or to double exponential for two compounds mixtures. From fitting results we can estimate the fluorescence lifetimes τ of the samples.

Before use the measured signals in any deconvolution method, they are first filtered to suppress undesired noises. The algorithm developed for noise filtering uses cursors resources of LabView. When this cursor facilities are used inside a while loop, it is possible to observe graphically the process results for different positions of the cursors. While the cursors in a graph are displaced, in other graph the process results are shown continuously. The filtering algorithm transforms the time-domain signals to frecuency-domain and a band-pass is selected by means of the cursors. The algorithm is described in following lines:

  open a file with data t_n, $f(t_n)$ and $y_o(t_n)$, assign signals data to program variables f and yo ;
  graph yo in a Waveform Graph "signals" (left graphs of figure 24) ;
  obtain Fourier transforms of both signals: FFT{f} and FFT{yo}, using Real FFT.vi ;
  graph FFT{yo} in XY Graph "FFT Real Mag" (right graphs of figure 24) ;
  while (ok filter = off)   ; while loop for dynamic processing, see figure 23
    read cursors positions in "FFT Real Mag" (blue traces in right graphs of figure 24) using
      property nodes, and find minimum and maximum x-indexes ;
    Cutoff.vi ; this subVI uses array functions to create a sub array with only the elements
      which are located between the cursor x-indexes, this means a cutoff of the signal
      outside the cursors positions. In graph "FFT Real Mag" x axes corresponds to
      frequency, thus the band-pass of the filter is the zone between cursors. The filtering
      process corresponds to a cut-off operation of the frequency spectrum.
    yo-filter = inverse Fourier transform of that part of the signal located between the cursors;
    graph yo and yo-filter in "signals" (left graphs in figure 24)

During while loop the cursors can be moved through the frequency-domain graph "FFT Real Mag". The effect of cursors displacement (select band-pass frequencies) can be observed continuously in time-domain graph "signals". This allows comparing the original and filtered signals dynamically. Figure 24 shows the result in time-domain (left graphs) for two different frequency band-pass (right graphs).

The instrumental response $f(t_n)$ is also filtered with the same band-pass selected with cursors. The filtering loop ends when the control "ok filter" on front panel is pressed.

After deconvolving by FFT, the useful information of the intrinsic fluorescence to be fitted is contained from its peak value to a minimum positive value. To cutoff signal in time-domain,
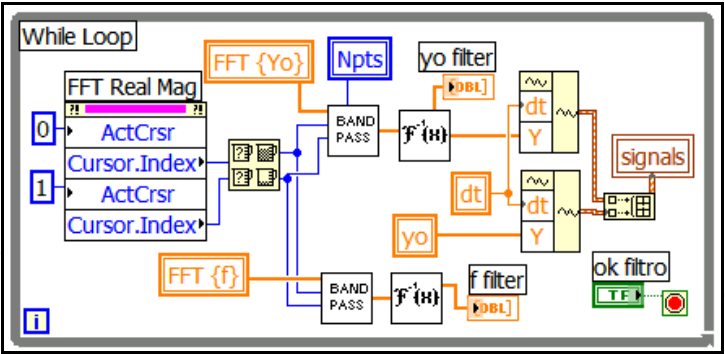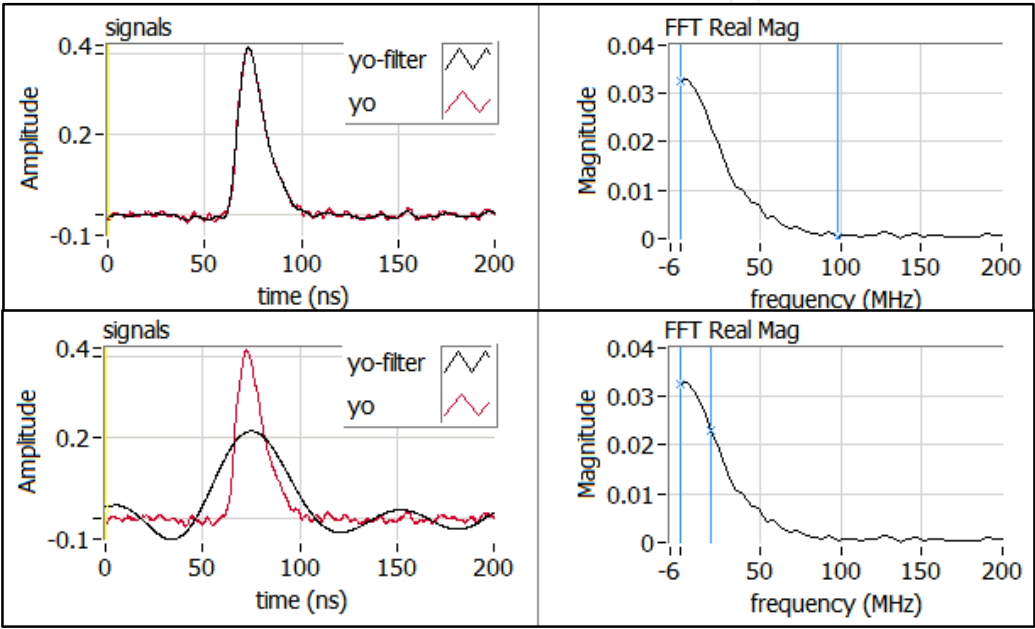
Fig. 23. Filtering process with cursors

Fig. 24. Signals during filtering process

we use another while loop with dynamic cursors performance similar to that of figure 23. For fitting process we use the Levenberg-Marqurdt algorithm, which is already provided by LabVIEW as a SubVI. We assume a single exponential for a simple fluorophore, and double exponential for a two components mixture. The goodness of fit is tested by means of residuals of equation (20), where $y_c(t_n)$ is the fluorescence computed by convolving the best fit found for $h(t_n)$ and the instrumental response $f(t_n)$. Figure 25 shows the result for rhodamine6G at 565 nm.

The program for data analysis by Laguerre deconvolution technique uses the filtered signals and computes the Laguerre functions according to equation (18). The number of functions L and Laguerre coefficient α are given as known values. The algorithm sequence is as follows:

    generate a set of Laguerre functions for given values of L and α, from equation (18)

    computes $\upsilon_j(t_n)$ from equation (20)

    ensemble the set of equations which minimize the sum of residuals Φ for coefficients c_j

    adjust variables to the same time-length ; use of while sentence with dynamic cursors

    c_j = Solve Linear Equations.vi   ;LabVIEW function to find c_j coefficients

    computes $h(t_n)$ from equation (17)

    computes $y_c(t_n)$ from convolution of equation (15)

    computes residuals $\Phi(t_n)$ from equation (21)   ; $\Phi(t_n)$ = square error(t_n)

Levenberg Marqurdt.vi   ;approximation to a simple exponential for a single fluorophore and to bi-exponential for two compounds mixtures to estimate fluorescence lifetimes
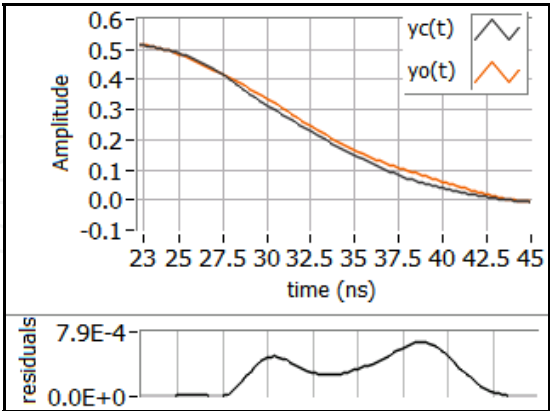

Fig. 25. Observed fluorescence and best fit

The analysis results are presented in terms of the fluorescence decay observed $y_o(t_n)$ and the fluoresce computed $y_c(t_n)$ with the best fit of the intrinsic fluorescence $h(t_n)$, as in figure 25. For a single fluorophore we use L=2 and for the mixtures L=3, α values were varied from 0.65 to 0.85.

4.4 Results

The performance of both deconvolution techniques FFT and LF is tested by means of the relative error (re), between reference value and the estimated lifetime, and the normalized mean square error (nmse). Table I summarizes the results obtained for each fluorophore at maximum emission peak wavelength, and table II summarizes the results for the mixtures, also at maximum emission peak wavelength. In tables refv is reference value from literauture, and estv is estimated value. From values in table I we observed that Laguerre expansion produces the best approximation for all fluorophores, with relative errors < -1%, and nmse values < 0.4%. Also, for mixtures in table 2 the best approximation is produced by

	refv (ns)	FFT			Laguerre		
		estv (ns)	re (%)	nmse (%)	estv (ns)	re (%)	nmse (%)
Fluoresceíne	4.01	4.12	2.23	1.15	3.99	-0.49	0.39
Rhodamine 6G	4.08	4.24	3.92	0.11	4.05	-0.73	0.09
Rhodamine B	1.68	1.59	-5.35	0.80	1.67	-0.12	0.24

Table 1. Results obtained for each fluorophore

	FFT					Laguerre				
	estv (ns)		re (%)		nmse (%)	estv (ns)		re (%)		nmse (%)
	$\tau 1$	$\tau 2$	$\tau 1$	$\tau 2$		$\tau 1$	$\tau 2$	$\tau 1$	$\tau 2$	
f-r6G	3.92	4.17	-2.24	2.2	1.68	3.96	3.98	-1.25	-2.45	0.42
f-rB	4.03	1.49	0.49	-11.3	4.66	4.02	1.58	0.25	-5.95	0.86
r6G-rB	4.21	1.56	3.18	-7.14	2.56	4.08	1.71	0.12	1.78	0.82

Table 2. Results obtained for each mixture

Laguerre deconvolution technique, with relative errors < -1.25% for τ_1 and < -6% for τ_2. The nmse values are < 1%.

5. Conclusions

In this work we developed an automated spectrofluorometer prototype, which is able to perform time-resolved fluorescence measurements. The pulsed light source is a home made nitrogen laser, which generates UV pulses (337.1 nm) at 30 Hz rates, with FWHM = 2.75 ns. We use a monochromator from Acton Research Corp., model SpectraPro 275 which includes a microprocessor control to receive commands from a computer via a serial RS-232 port for scan control. To detect the fluorescence emitted by the sample, we use the PMT module H7732P-11 manufactured by Hamamatsu, which contains a high sensitivity photomultiplier tube with a peak radiant sensitivity of 80 mA/W at 430 nm, and 2 ns characteristic rise-time. To detect the laser pulse we use the fast photodiode MRD500 with a response time of 1 ns on 50 Ω load, and a sensitivity of 1 nA/mW/cm2 at 337.1 nm.

To measure the excitation pulse laser and the fluorescent response pulse, we use a digital oscilloscope model 2440 from Tektronix®. This oscilloscope has 300 MHz analog input bandwidth and 1 MΩ input impedance. This impedance can be programmed to be 50 Ω, as it is needed to measure the current signals coming from the photodetectors. The oscilloscope operation is programmed from a computer via its GPIB port. We use the interface board GPIB-USB-HS from National Instruments, which is directly connected to the oscilloscope and communicates with a computer via USB interface. For the complete spectrometer, we determine the characteristic rise-time of the instrumental (5.647 ns) and its temporal resolution (FWHM = 13.28 ns). This slowing of the input signal is mainly caused by the monochromator.

A control and acquisition program was developed in the graphical language G of LabVIEW 7.1 environment. This program controls the monochromator to generate a wavelength (λ) sweep, and reads the information of the time-resolved signals (excitation and response) measured by the oscilloscope in each λ value. The program was designed to execute one of three main functions: *GoTo/Measure Noise*, *Sweep*, and *Open Files*. With this program we measured the fluorescence emitted by 3 substances with well known fluorescence life-times: fluoresceine, rhodamine 6G and rhodamine B. Also we measured the fluorescence emitted by 3 mixtures of two fluorophores. For each fluorophore and mixture, were performed 6 wavelength sweeps from 400nm to 700nm with 5nm increments.

A data analysis program was developed in LabVIEW 7.1 to estimate the intrinsic fluorescence decay from deconvolution of measured signals. The program applies two deconvolution techniques: Fast Fourier transform and Laguerre expansion. The intrinsic fluorescence obtained with both methods is fitted to a simple exponential for a single fluorophore, or to double exponential for two compounds mixtures. From fitting results we can estimate the fluorescence lifetimes τ of the samples. LabVIEW provides an easy access to cursor resources. When these cursor facilities are used inside a while loop, it is possible to observe graphically the process results for different positions of the cursors. While the cursors in a graph are displaced, in other graph the process results are shown continuously. We used this while loop with dynamic cursors inside, to perform filtering, shifting, and cutting of signals.

From data analysis results, deconvolution by Laguerre expansion provides a good approximation with nmse values < 0.4% for single fluorophore and < 1% for mixtures. The Laguerre functions have been suggested as an appropriate orthonormal basis owing to their buil-in exponential term that makes them suitable for physical systems with asymptotically exponential relaxation dynamics (Jo et all, 2004). Because the Laguerre basis is a complete

orthonomal set of functions, a unique characteristic of this approach is that it can reconstruct a fluorescenece response of arbitrary form. Laguerre deconvolution technique is a suitable approach for the analysis of time-domain fluorescence data of complex systems, since this technique has the ability to expand intrinsic fluorescence of any form, without any a priori assumption of its functional form.

6. References

Anderson, J.; Fischer, R.; Smith, C.; Webb, S. & Dennis, J. (2003). In situ detection of pathogen indicators using laser-induced fluorescence, *Proccedings of 2003 UCOWR Annual Conference "Water Security in the 21st Century"*, http://ucowr.siu.edu/proc/W1C.pdf.

Ardizzoni, J. (2007). High-Speed Time-Domain Measurements – Practical Tips for Improvement, Analog Dialogue, March 2007, 41-03.

Geddes, Ch. D. & Lakowicz, J. R. (2004). Lakowicz, *Reviews in Fluorescence 2004*, Kluwer Academic/Plenum Publishers, 0-306-48672-5 (eBook), New York, USA.

Gore, M.G. (2000). *Spectrophotometry and Spectrofluorimetry*, Oxford University Press, 2nd Edition, 0-19963812-8, New York, USA.

Jo, J.; Fang, Q.; Papaioannou, T. & Marcu, L. (2004). Fast model–free deconvolution of fluorescence decay for analysis of biological systems, *Journal of Biomedical Optics*, 9(4), 743 – 752.

Lakowicz, J. R. (1991). *Topics in Fluorescence Spectroscopy, Volume 1: Techniques,* Plenum Press, 0-3064-3874-7, New York, USA.

Lakowicz, J. R. (1999). *Principles of Fluorescence Spectroscopy*, Klumer Academic/Plenum Publishers, 2nd Edition, 0-306-46093-9, New York, USA.

Lawton, R.; Riad, S. & Andrews, J. (1986). Pulse and Time- Domain Measurements,. *Proc. IEEE, Vol.74, Jan. 1986*, 77-81.

Maarek, J-M.I.; Marcu, L.; Snyder, W.J. & Grundfest, W.S. (2000). Time-resolved Fluorescence Spectra of Arterial Fluorescent Compounds: Reconstruction with the Laguerre Expansion Techique, *Photochemistry and Photobiology*, 71, 178-187.

Moller, C. & Mortensen, G. (2008). Fluorescence spectroscopy; a rapid tool for analyzing dairy products, *J. Agric. Food Chem.*, 56, 720-729.

Nahman, N.S. (1978). Picosecond-Domain Waveform Measurements, *Proceedings of IEEE, Vol. 66, No.4*, April 1978, 441-454.

Nesterenko, T.V.; Tikhomirov, A.A. & Shikhov, V.N. (2007). Chlorophyll fluorescence induction and estimation on plant resistance to stress factors, *Zh. Obshch Biol.*, 68, 444-458.

O´Connor, D.V. & Ware, W.R. (1979). Deconvolution of fluorescente decay curves. A critical comparison of techniques, *The Journal of Physical Chemistry*, 83, 1333-1343.

Paras, N. P. (2003). *Introduction to Biophotonics*, Jhon Wiley&Sons, Inc., 0-471-28770-9, New Jersey.

Poulli, K.I.; Mousdis, G.A. & Georgiou, C.A. (2007). Rapid synchronous fluorescence method for virgin olive oil adulteration assessment, *Food Chemistr*, 105, 369-375.

Spring, K.R.; Fellers T.J. & and Davidson, M.W. (2010). Introduction to Charge-Coupled Devices (CCDs), Nikon Microscopy Fundamentals of Digital Imaging http://www.microscopyu.com/articles/digitalimaging/ccdintro.html

Valeur, B. (2002). *Molecular Fluorescence: Principles and Applications*, Wiley-BCH-Verlag, 3-527-29919-X, Federal Republic of Germany.

Vo-Dinh, T. (2003). *Biomedical Photonics Handbook*, CRC Press, 0-8493-1116-0, Florida, USA

Weller, D. (2002). Relating wideband DSO rise time to bandwidth: Lose the 0.35, *EDN*, Dec. 12, 2002, 89-94.
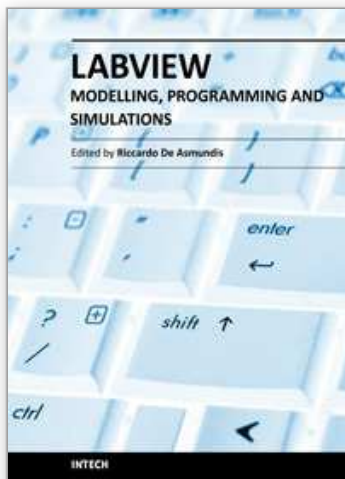
Modeling, Programming and Simulations Using LabVIEW™ Software

Edited by Dr Riccardo De Asmundis

Born originally as a software for instrumentation control, LabVIEW became quickly a very powerful programming language, having some characteristics which made it unique: simplicity in creating very effective User Interfaces and the G programming mode. While the former allows for the design of very professional control panels and whole applications, complete with features for distributing and installing them, the latter represents an innovative way of programming: the graphical representation of the code. The surprising aspect is that such a way of conceiving algorithms is extremely similar to the SADT method (Structured Analysis and Design Technique) introduced by Douglas T. Ross and SofTech, Inc. (USA) in 1969 from an original idea by MIT, and extensively used by the US Air Force for their projects. LabVIEW enables programming by implementing directly the equivalent of an SADT "actigram". Apart from this academic aspect, LabVIEW can be used in a variety of forms, creating projects that can spread over an enormous field of applications: from control and monitoring software to data treatment and archiving; from modeling to instrument control; from real time programming to advanced analysis tools with very powerful mathematical algorithms ready to use; from full integration with native hardware (by National Instruments) to an easy implementation of drivers for third party hardware. In this book a collection of applications covering a wide range of possibilities is presented. We go from simple or distributed control software to modeling done in LabVIEW; from very specific applications to usage in the educational environment.

How to reference

In order to correctly reference this scholarly work, feel free to copy and paste the following:

INTECH
open science | open minds

www.intechopen.com

Fax: +385 (51) 686 166
www.intechopen.com

Fax: +86-21-62489821